

## Supplementary Material

### **A Transferrin-Conjugated Hollow Nanoplatfom for Redox-Controlled and Targeted Chemotherapy of Tumor with Reduced Inflammatory Reactions**

Jun Zhou,<sup>1,‡</sup> Menghuan Li,<sup>1,‡</sup> Wei Qi Lim,<sup>2,‡</sup> Zhong Luo,<sup>1,3,\*</sup> Soo Zeng Fiona Phua,<sup>2</sup> Runlan Huo,<sup>1</sup> Liqi Li,<sup>4</sup> Ke Li,<sup>3</sup> Liangliang Dai,<sup>3</sup> Junjie Liu,<sup>3</sup> Kaiyong Cai,<sup>3</sup> Yanli Zhao<sup>2,5,\*</sup>

1. School of Life Science, Chongqing University, Chongqing 400044, P. R. China.
2. Division of Chemistry and Biological Chemistry, School of Physical and Mathematical Sciences, Nanyang Technological University, 21 Nanyang Link, Singapore 637371.
3. Key Laboratory of Biorheological Science and Technology, Ministry of Education, Chongqing University, Chongqing 400044, P. R. China.
4. Department of General Surgery, Xinqiao Hospital, Third Military Medical University, Chongqing 400037, China.
5. School of Materials Science and Engineering, Nanyang Technological University, 50 Nanyang Avenue, Singapore 639798.

<sup>‡</sup>These authors contributed equally to this work.

E-mail: zhaoyanli@ntu.edu.sg; luozhong918@cqu.edu.cn

**Materials:** All reagents mentioned in the text above were obtained from Sigma-Aldrich and used as received. Nude mice (average weight:  $18.4 \pm 0.6$ g) were provided by Xingqiao Hospital of The Third Military Medical University (Chongqing, China) for the animal study, which were conducted strictly under the Animal Management Rules of the Ministry of Health of the People's Republic of China (Document No. 55, 2001) and the guidelines for the Care and Use of Laboratory Animals of The Third Military Medical University.

**Characterizations:** SEM and TEM characterizations were conducted on JSM-7800F (JEOL, Japan) and ZEISS LIBRA 200F (ZEISS, Germany) at the acceleration voltages of 30 and 100 kV, respectively. The release profile was recorded in a real-time manner with a fluorospectrophotometer (RF5301PC, Shimadzu, Japan) with 1 cm quartz cells as containers. Confocal laser scanning microscopy (LSM 510 Meta, Zeiss Co., Germany) was used to determine the intracellular distribution of administered samples. Flow cytometry (Coulter Epice XL, Beckman Coulter, USA) was used to quantify the apoptosis of cancer cells after nanoparticle internalization. Plasma concentration of nanoparticles in mice after the intravenous administration was investigated with Thermo Scientific iCAP (7000 Series ICP-OES Duo). Regarding the histological inspection of major organs and tumor tissues, representative samples were extracted from the host and frozen-sliced into sections of appropriate thickness (Leica CM1950, Germany). The observation of the cross-sectioned samples was done on CLSM (510 Meta, Germany).

### **Methods:**

**Preparation of HMSNs.** The procedure for the synthesis of HMSN was adapted from previous reports.<sup>S1,S2</sup> Dense  $\text{SiO}_2$  nanoparticles and surfactant-protected  $\text{SiO}_2$ @CTAB- $\text{SiO}_2$  core/shell nanoparticles were firstly prepared as precursors. Briefly, tetraethoxysilane (TEOS, 10 mL) and ammonium hydroxide (10 mL) were dissolved into a mixture solution of ethanol/water (428mL/60mL, v/v) with gentle stirring at 30 °C for 2 h. After centrifugation, the white product was rinsed with ethanol and distilled water in turn for 4 times. Finally, the sample was sonicated and dispersed into distilled water for the preparation of core/shell silica nanoparticles. Firstly,  $\text{SiO}_2$  nanoparticles (100 mg) were dispersed into distilled water (20 mL) under ultrasonication for 30 min. Then, the white solution was added to a mixture solution containing CTAB (150 mg), deionized water (30 mL), ethanol (30 mL), and concentrated ammonia solution (0.55 mL). After stirring at room temperature for 30 minutes, TEOS (0.25 mL) was quickly added to the mixture solution. The reaction would continue for another 6 h and the precipitates were collected by centrifugation, rinsed with ethanol and water for 4 times, and then re-dispersed into distilled water (20 mL), which was denoted as  $\text{SiO}_2$ @CTAB- $\text{SiO}_2$ . Finally, to obtain HMSNs, the  $\text{SiO}_2$  core and CTAB were removed using  $\text{Na}_2\text{CO}_3$ . The  $\text{SiO}_2$ @CTAB- $\text{SiO}_2$  suspension was first sonicated for 20 min and vigorously stirred for another 4 h. Subsequently,  $\text{Na}_2\text{CO}_3$  (470 mg) was added into the suspension and

stirred at 50 °C for another 10 h. After centrifugation and extensive washing with water, the product was re-dispersed into the mixture of methanol and HCl (50 mL/4mL, v/v) to extract CTAB. After refluxed at 80 °C for 24h, the product was finally collected by centrifugation and extensively washed with deionized water and ethanol, which was denoted as HMSNs.

**Preparation and characterization of transferrin-capped HMSNs.** To construct transferrin-functionalized HMSNs, disulfide bond was used as the linkage to immobilize transferrin moieties onto the pore-openings of HMSNs. The preparation procedures were briefly described in four steps.

The as-prepared HMSNs were firstly grafted with sulfhydryl groups on their surface. Specifically, unmodified HMSNs (0.2 g) were dried and then refluxed with 3-mercaptopropyltrimethoxysilane (0.5 mL) in anhydrous toluene (50 mL) at 60 °C for one day. The product was collected through centrifugation and then repetitively purified with ethanol and acetone, which was denoted as HMSNs-HS.

Subsequently, HMSNs-HS (0.5 g) was re-dispersed in ethanol (30 mL) and added with acetic acid (1.2 mL) and then 2-carboxyethyl-2-pyridyldisulphide (0.5 g). The mixture was rigorously stirred at 20 °C and reacted for 48 h. The extracted product was washed first with ethanol and then deionized water for three times each, and eventually anhydrated in high vacuum at 30 °C. The resultant nanoparticles were denoted as HMSNs-S-S-COOH.

For the grafting of pentynoic acid, HMSNs-S-S-COOH (0.5 g) were redispersed in N,N-dimethylformamide (DMF, 50 mL) and vigorously stirred for 6 h. The temperature of the mixture was maintained at 45 °C. 1-(3-Dimethylaminopropyl)-3-ethylcarbodiimide hydrochloride (EDC, 0.3g) and N-hydroxysuccinimide (NHS, 0.19g) were added to the mixture and reacted for 6 more hours, during which the solution was continuously stirred with a magnetic stirrer. The nanoparticles were extracted via centrifugation and redispersed into DMF (50 mL) solution after washing. But-3-yn-1-amine hydrochloride (0.5 mL) was then added to the mixture and mildly stirred at room temperature for 24 h. During this process, the COOH groups of the HMSNs-S-S-COOH reacted with the NH<sub>2</sub> group in but-3-yn-1-amine hydrochloride, thus realizing the conjugation of the alkynyl end groups. The extracted nanoparticles were then washed with ethanol and deionized water for three times each, and anhydrated in high vacuum at room temperature. The resultant sample was denoted as HMSNs-S-S-C≡C.

HMSNs-S-S-C≡C was functionalized with azide-functionalized transferrin to introduce the cancer specificity. For the azidization of transferrin, 2-azidoacetic acid (10 μL) was dissolved into aqueous buffer (5 mL) in which the pH has been tuned to 5.5, followed by the addition of aqueous buffer (1 mL) containing EDC/NHS (5mg/3mg). The reaction was lasted for 8 h. Afterwards, the reaction mixture was added dropwise to the transferrin solution (600mg of transferrin dispersed in 20 mL aqueous buffer) and reacted for 24 hours more at 4 °C. When the reaction was complete, the mixture would be dialyzed (Mn: 3000) against deionized water for 48 h to remove the residual EDC, NHS and 2-azidoacetic acid. The

azide-modified transferrin obtained in this step was anhydrous by lyophilization and denoted as Tf-N<sub>3</sub>.

For the loading of DOX, HMSNs-S-S-C≡C (20 mg) and DOX (30 mg) were extensively mixed in deionized water (12 mL) and stirred for 24 h, so that DOX would be concentrated in the mesopores through passive diffusion and capillary effect. After the loading of DOX, the aqueous solution (1 mL) of Tf-N<sub>3</sub> (20 mg), CuSO<sub>4</sub> (2 mg) and ascorbic acid (5 mg) would be added to the solution containing the nanoparticles. The click reaction for the Tf conjugation was conducted under N<sub>2</sub> protection and lasted for 24 h. The sample was collected by centrifugation and washed with deionized water for four times, followed by vacuum freeze-drying. The product of this step was denoted as HMSNs-S-S-Tf@DOX. The drug entrapment efficiency (DEE) of DOX was calculated through the following formula: DEE (%) = amount of loaded drug / amount of totally added drug. For some tests DOX was not added before the click reaction, and those products were denoted as HMSNs-S-S-Tf.

Alternatively, for some optical characterizations FITC (10 mg) were used for the cargo loading instead of DOX. Consequently, the sample was denoted as HMSNs-S-S-Tf@FITC. The intermediates and final product were fully characterized.

**Redox-responsive drug release from HMSNs-S-S-Tf.** The redox-initiated drug release mechanism of HMSNs-S-S-Tf was investigated with GSH as the stimulant and DOX was used as a model drug to indicate the percentage of cargo release. The accumulative DOX release from HMSNs-S-S-Tf @DOX was monitored by fluorospectrophotometer.

**Cell culture.** MDA-MB-231 cells and macrophage cells were cultured in DMEM and RPMI1640 media, which contained 10% FBS (Gibco), penicillin (100U mL<sup>-1</sup>) and streptomycin (100 µg mL<sup>-1</sup>). The incubated was set to 37 °C with a 5% CO<sub>2</sub> atmosphere. The cell culture media were replaced with new ones every other day. Then, BREAST CANCER cells were seeded into cell culture flasks or 24-well plates at an initial cell density of 2 × 10<sup>4</sup> unit/cm<sup>2</sup>. As soon as the cell confluence reached 60~70%, the medium was refreshed with new ones in which HMSNs, HMSNs-S-S-Tf, DOX, and HMSNs-S-S-Tf@DOX have been added respectively.

**TEM characterization for the intracellular distribution of the nanoparticles.** To visualize the intracellular distribution of the nanoparticles, Breast cancer cells were firstly incubated under normal conditions, HMSNs (70 µg mL<sup>-1</sup>), and HMSNs-S-S-Tf (70 µg mL<sup>-1</sup>) for 24 h, respectively. The TEM samples were prepared through the protocol established in previous reports. Cells were first detached and fixed by the mixture of glutaraldehyde (2% w/v) and paraformaldehyde (2% w/v) at 4 °C for 2 h. Subsequently, the cell samples were purified with cacodylate buffer for three more times. The samples were post-fixed by osmic acid (2%) for 15 min and stained by uranyl acetate for 15 min more. The stained cells were then dehydrated by ethanol/water mixture of graded concentrations, followed by incubation with the mixture of anhydrous ethanol and Spurr's medium (1:1, v/v) for 1 h. The incubated sample cells were processed under vacuum at 60 °C overnight and sliced into ultrathin sections using a

microtome, then again stained by uranyl acetate for 5 min. The allocation of internalized HMSNs-S-S-Tf was observed by TEM.

**CLSM characterization of the nanoparticle distribution within MDA-MB-231 or macrophage cells.** For the CLSM characterization of the intracellular distribution of nanoparticles, MDA-MB-231 or RAW264.7 macrophage cells were incubated with FITC, HMSNs@FITC, and HMSNs-S-S-Tf@FITC (all samples had an equivalent FITC concentration of  $70 \mu\text{g mL}^{-1}$ ), respectively. After culturing at  $37^\circ\text{C}$  for either 12 or 24 h, trypan blue ( $200 \mu\text{g mL}^{-1}$ ) was added to quench the cytoplasmic fluorescence. The cell samples were then fixed by 2% glutaraldehyde for 20 min and permeabilized with 0.2% Triton X-100 for 2 min, while the ambient temperature were maintained at  $4^\circ\text{C}$ . The fixed cells were later stained with rhodamine-phalloidin ( $5 \mu\text{g mL}^{-1}$ ) at  $4^\circ\text{C}$  overnight. For the visualization of the cell nuclei, Hoechst 33258 ( $10 \mu\text{g mL}^{-1}$ ) were also used for the staining and the treatment lasted 5 min. The processed samples were eventually mounted with 90% glycerinum and observed by CLSM.

**Cytotoxicity assay by MTT.** The culture medium was renewed with new ones containing different concentrations of HMSNs, HMSNs-S-S-Tf, DOX, and HMSNs-S-S-Tf@DOX, respectively, when the cell confluence of all plates reached 60~70%. The temperature for the incubation was set to  $37^\circ\text{C}$ . After incubation for 6, 12, and 24 h, respectively, the old media were replaced by fresh unmingled ones. MTT solution ( $0.1\text{mL}$ ,  $5\text{mg mL}^{-1}$ ) was added to each well, and the incubation would last for 4 more hours. For the measurement of optical densities, the MTT-containing medium was pipetted away carefully, and dimethyl sulfoxide ( $0.5 \text{ mL}$ ) was added to dissolve the emerging formazan dye crystals. After mild shaking, the optical density for each well was measured by the enzyme-linked immunosorbent assay (ELISA) under 490 nm.

**Cell apoptosis assay by flow cytometry.** To evaluate the extent of cell apoptosis (%) after the internalization of HMSNs-S-S-Tf@DOX, MDA-MB-231 cells were cultured on a 24-well plate at an initial seeding density of  $2 \times 10^4$  cells/cm<sup>2</sup>. HMSNs, HMSNs-S-S-Tf, DOX, and HMSNs-S-S-Tf@DOX were added using the same setup as mentioned above. After incubation with nanoparticles, the cells were extracted through centrifugation and rapidly washed twice with PBS before the staining. The apoptosis/death cell assay kit (Invitrogen) was used strictly under the protocol provided by the manufacturer. Annexin V-FITC was used for the staining of cells in the apoptotic state. Flow cytometric analysis was eventually performed on a BD FACS Calibur Flow Cytometer, and the results were analyzed by FlowJo Ver. 10.0.

**Flow cytometry characterization for the distribution of nanoparticles within MDA-MB-231 or macrophage cells.** MDA-MB-231 or RAW264.7 macrophage cells were incubated with FITC, HMSNs@FITC, and HMSNs-S-S-Tf@FITC (all samples had an equivalent FITC concentration of  $70 \mu\text{g mL}^{-1}$ ), respectively. After culturing at  $37^\circ\text{C}$  for either 12 or 24 h, trypan blue ( $200 \mu\text{g mL}^{-1}$ ) was added to quench the cytoplasmic fluorescence. Then

these cells in each sample were collected by digestion and rinsed with PBS by centrifugation. At last, Flow cytometric fluorescence intensity analysis was eventually performed on a BD FACS Calibur Flow Cytometer, and the results were analyzed by FlowJo Ver. 10.0.

**Distribution of nanoparticles within MDA-MB-231 or macrophage cells by ICP characterization.** MDA-MB-231 or RAW264.7 macrophage cells were incubated with PBS, HMSNs and HMSNs-S-S-Tf, respectively. After culturing at 37 °C for either 12 or 24 h, cells in each sample were collected by digestion and rinsed with PBS by centrifugation. Then each sample was treated with lysis buffer (1% SDS, 1% Triton X-100, 40 mM Tris acetate, 0.5 mL) for cell disintegration. HF (0.5 mL) was then added to dissolve the HMSNs into Si<sup>4+</sup> ions. After 5 min of centrifuging at 1000 rpm, the Si concentration in cells was measured by ICP on iCAP 6300 Duo.

**Biodistribution of HMSNs and HMSNs-S-S-Tf in major mouse organs and tumors by ICP.** Healthy nude mice (six mice per group) were intravenous injected with HMSNs and HMSNs-S-S-Tf (100 µL, 1 mg mL<sup>-1</sup>). These mice were sacrificed one day after injection. For biodistribution measurement, major organs including heart, liver, spleen, lungs, kidneys as well as tumors were surgically extracted and treated by lysis buffer (1% SDS, 1% Triton X-100, 40 mM Tris acetate, 1 mL) and HF (1 mL) after trituration treatment. After 5 min of centrifuging at 1000 rpm, the Si concentration in each sample was measured by ICP on iCAP 6300 Duo.

**Long term biodistribution of HMSNs-S-S-Tf in major mouse organs and tumors by ICP:** Healthy nude mice (six mice per group) were intravenously injected with HMSNs-S-S-Tf (100 µL, 1 mg mL<sup>-1</sup>), which were sacrificed 1 day, 7 days or 28 days after the injection. For the characterizations of biodistribution, major organs including heart, liver, spleen, lung, kidney as well as tumor were surgically extracted and treated by lysis buffer (1% SDS, 1% Triton X-100, 40 mM Tris acetate, 1 mL) and HF (1 mL) after trituration treatment. After 5 min of centrifuging at 1000 rpm, the Si concentration in each sample was measured by ICP on iCAP 6300 Duo.

**Plasma concentration of nanoparticles after administration by ICP.** Twelve mice were intravenously injected with HMSNs or HMSNs-S-S-Tf (0.1 mg per animal) and divided randomly into two groups of equal size. Blood (50 µL) was collected from the orbital sinus at different points in time and then added with lysis buffer (1% SDS, 1% Triton X-100, 40 mM Tris acetate, 0.5 mL). HF (0.5 mL) was then used to dissolve the HMSNs into Si<sup>4+</sup> ions. After 5 min of centrifuging at 1000 rpm, the Si concentration in the blood samples was measured by ICP on iCAP 6300 Duo, which were normalized and shown as the percentage of dose amount in a gram of serum (%ID g<sup>-1</sup>).

**Determination of inflammation cytokines after injection of nanoparticles in vivo.** The expression levels of interleukin-β (IL-β) and tumor necrosis factor-α (TNF-α) were measured using the procedures established in a previous study. To start with, twelve mice were intravenously injected with HMSNs or HMSNs-S-S-Tf (0.1 mg per animal). Blood (50 µL)

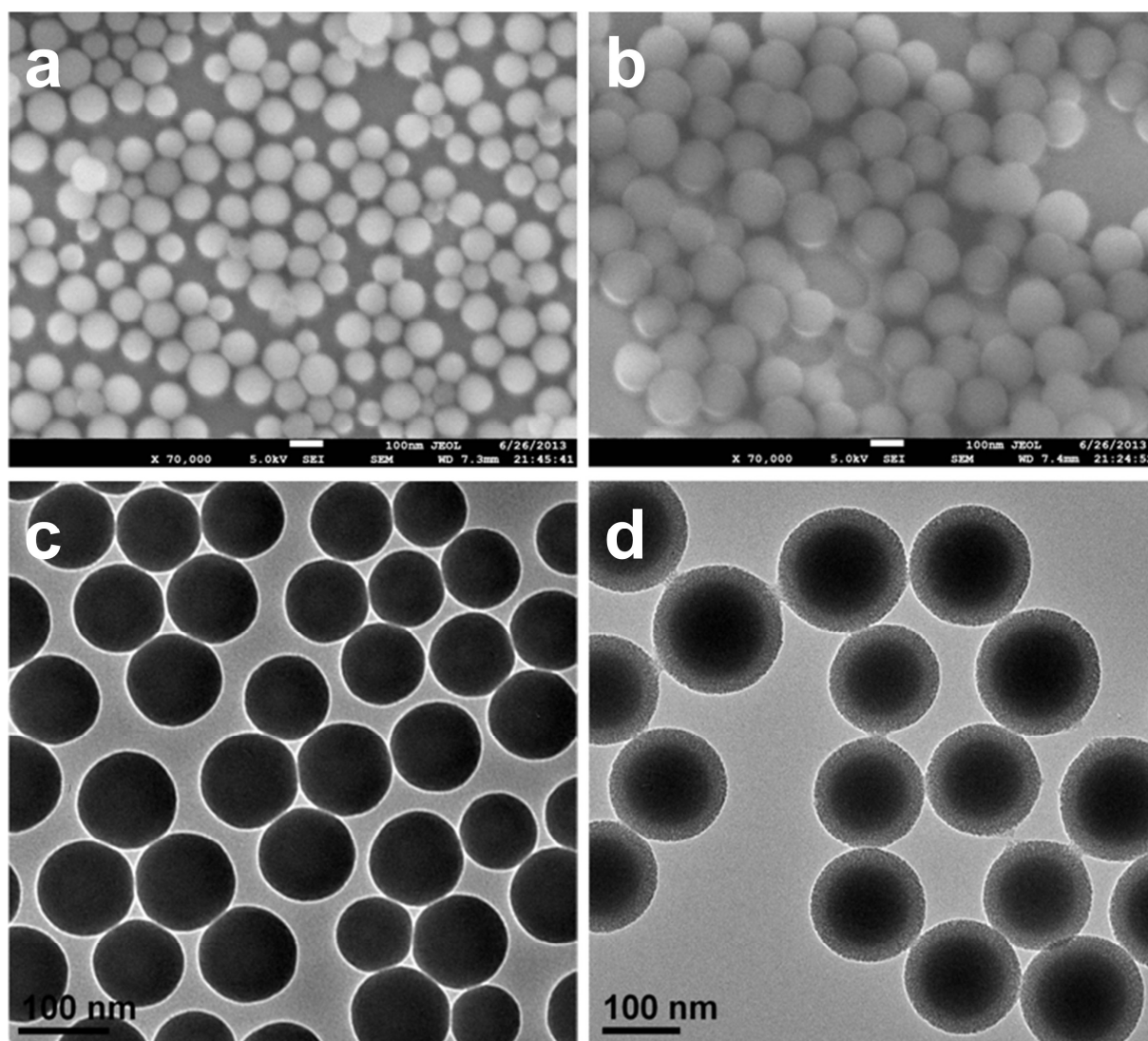
was collected from the orbital sinus at different points of time and then centrifuged at 2000 rpm for 10 min to extract the serum. The serum concentration of IL-1 $\beta$  and TNF- $\alpha$  were measured by enzyme-linked immunosorbent assay (ELISA) kit. The optical density of solution was recorded by a microplate reader (Bio-Rad 680, USA) at 450 nm.

**Establishing the mouse models of breast cancer.** MDA-MB-231 cells ( $0.2\text{mL}$ ,  $1.5\times 10^7$  cells  $\text{mL}^{-1}$ ) were dispersed in PBS and injected into the subcutaneous tissue of mice to establish the tumor. The treated mice were checked daily to investigate the size changes of tumors, which were measured with a digital caliper. When the average tumor volume reached around  $110\text{mm}^3$  (calculation: volume = (tumor length) $\times$ (tumor width) $^2/2$ ), all mice were ready for the subsequent studies. Mice with the greatest or the smallest size of tumors were excluded. Representative mice were picked out from which the tumor tissues were surgically extracted to study the tumor morphology.

**Chemotherapeutic treatment of the tumor-bearing mice.** In this part, lipoma tumors of comparable sizes were created on 60 mice, which were divided equally into five groups and intravenously injected three times per week with saline, HMSNs, HMSNs-S-S-Tf, DOX, and HMSNs-S-S-Tf@DOX, respectively. Mice treated with saline ( $100\ \mu\text{L}$ ) were used as the experimental control. The amount of HMSN-S-S-Tf@DOX injection was around  $0.1\ \text{mg}$  per animal ( $100\ \mu\text{L}$ ,  $1\ \text{mg}\ \text{mL}^{-1}$ ) each time, which is equivalent to  $0.02\ \text{mg}$  of DOX for each mouse ( $100\ \mu\text{L}$ ,  $0.2\ \text{mg}\ \text{mL}^{-1}$ ). The concentrations of HMSNs and HMSNs-S-S-Tf were kept the same as the HMSN-S-S-Tf@DOX group. After the injection of saline and nanoparticles, the tumor size on each mouse was measured by a digital caliper. Additionally, all mice were weighted using a digital balance. All surviving mice were sacrificed after three weeks, and the tumor tissues or major organs were extracted to study the tumor morphology or for other uses.

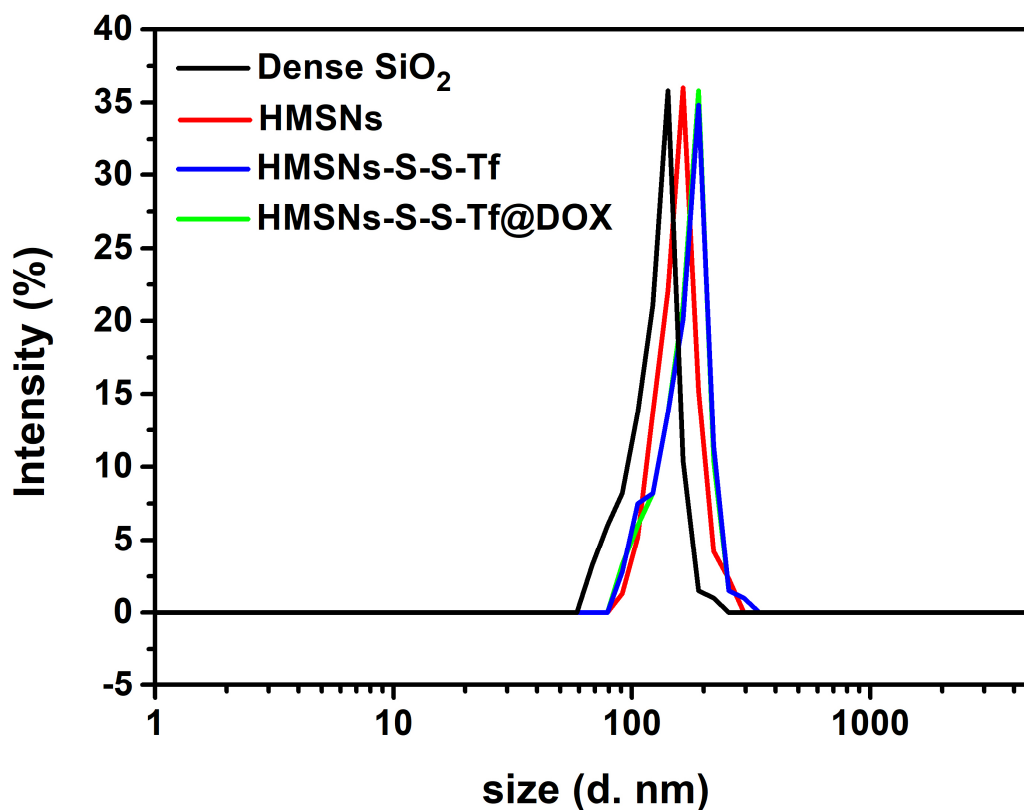
**Examination of pathological changes in tumor tissues and toxicity to major organs after administration.** To histologically examine the mouse samples, tumor tissues and major organs were surgically extracted from the host and treated with 10% formalin at  $4\ ^\circ\text{C}$  for two days. When the processing of all tissues was complete, they were embedded in paraffin and sliced into thin sections. The samples were stained with hematoxylin and eosin (H&E) and the cell nuclei were studied by CLSM.

**In Vivo NIRF Imaging.** 18 MDA-MB-231-tumor-bearing nude mice were randomly divided into three groups (six mice per group) and intravenously injected with saline, HMSNs@DOX and HMSNs-S-S-Tf@DOX ( $100\ \mu\text{L}$ ,  $1\ \text{mg}\ \text{mL}^{-1}$ ), respectively. Then, the mice were imaged using IVIS Lumina II at the excitation wavelength of  $479\ \text{nm}$  after 24 h. The average NIRF intensity at tumor was calculated and statistically compared.



**Figure S1.** Representative morphologies of nanoparticles. SEM images of (a) SiO<sub>2</sub> nanoparticles and (b) SiO<sub>2</sub>/CTAB-SiO<sub>2</sub> hybrid. Scale bar: 100 nm. TEM images of (c) SiO<sub>2</sub> nanoparticles and (d) SiO<sub>2</sub>/CTAB-SiO<sub>2</sub> hybrid. Scale bar: 100 nm.

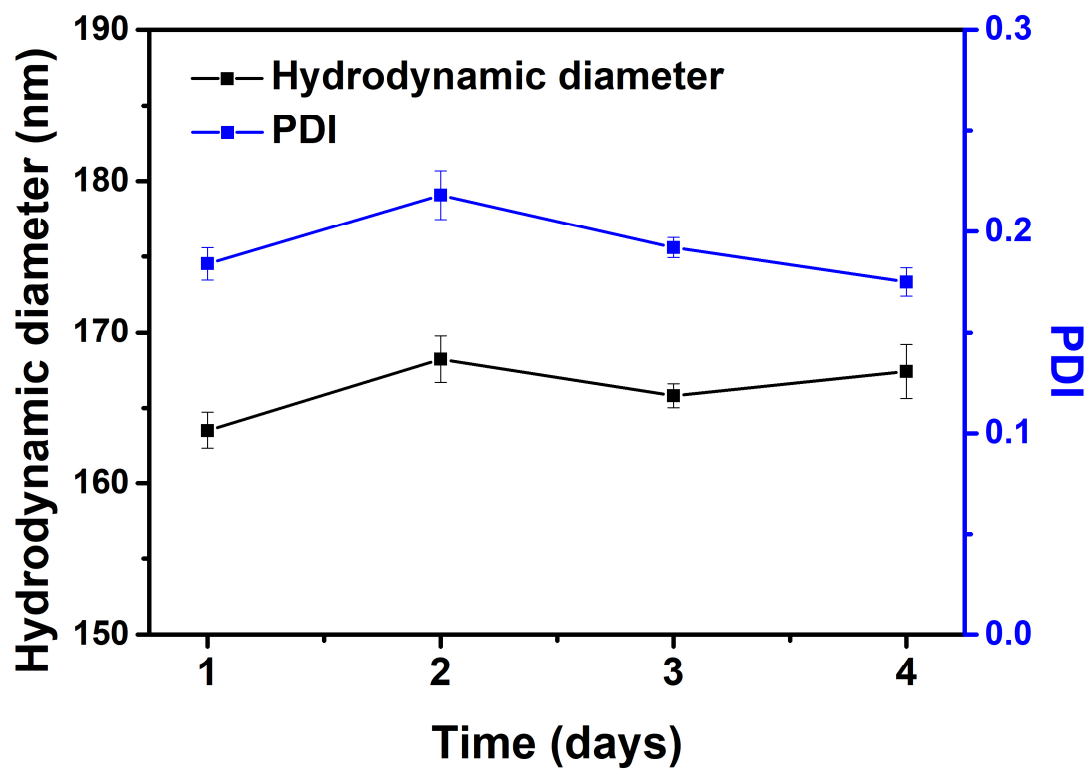




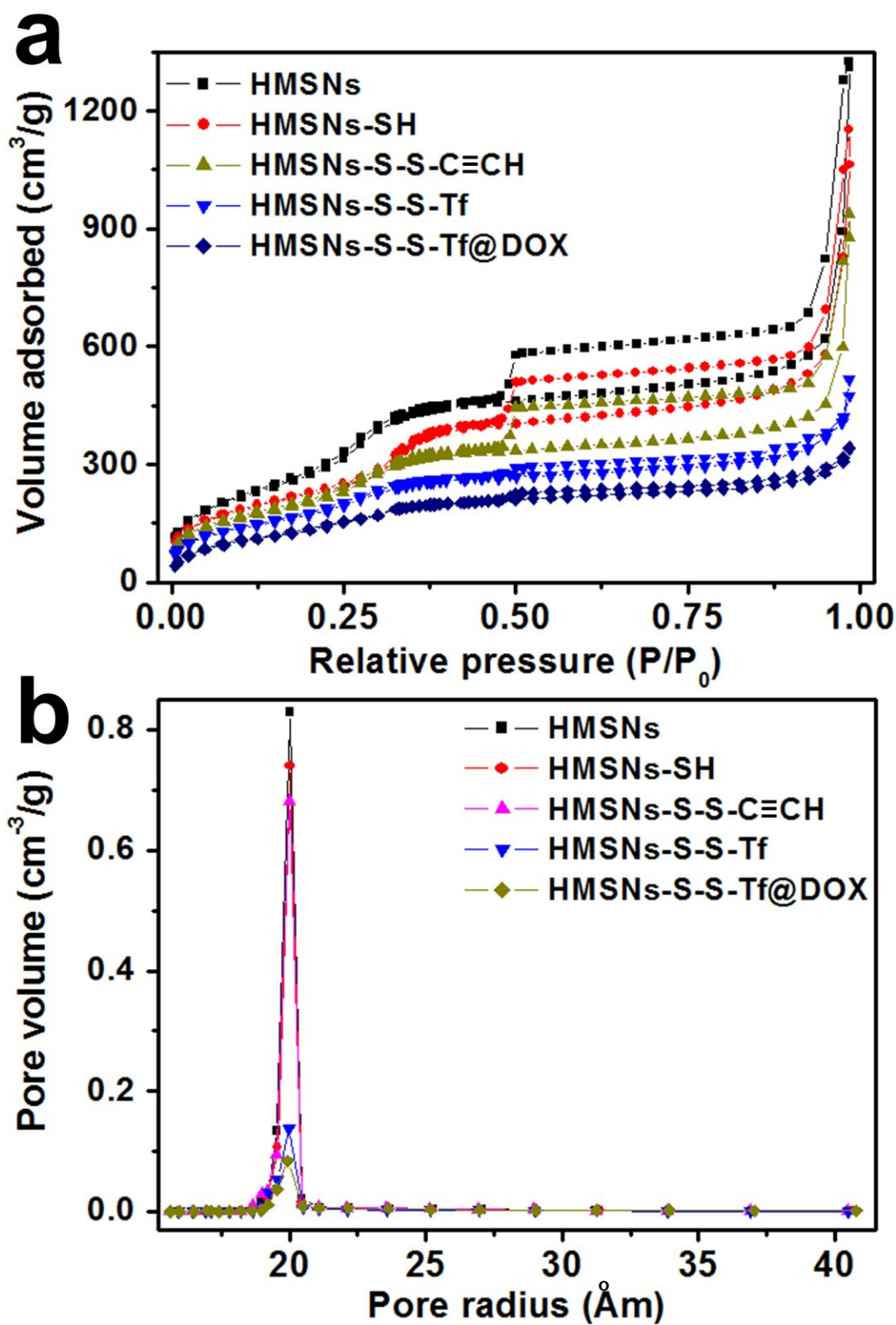
**Figure S2.** Size distribution of dense silica nanoparticles, HMSNs, HMSN-S-S-Tf and HMSNs-S-S-Tf@DOX *via* DLS.

**Table S1.** Polymer dispersity index (PDI) measurements for dense silica nanoparticles, HMSNs, HMSN-S-S-Tf and HMSNs-S-S-Tf@DOX.

Materials	Polymer dispersity index (PDI)
Dense SiO <sub>2</sub> nanoparticles	<b>0.274</b>
HMSNs	<b>0.231</b>
HMSNs-S-S-Tf	<b>0.165</b>
HMSNs-S-S-Tf@DOX	<b>0.167</b>



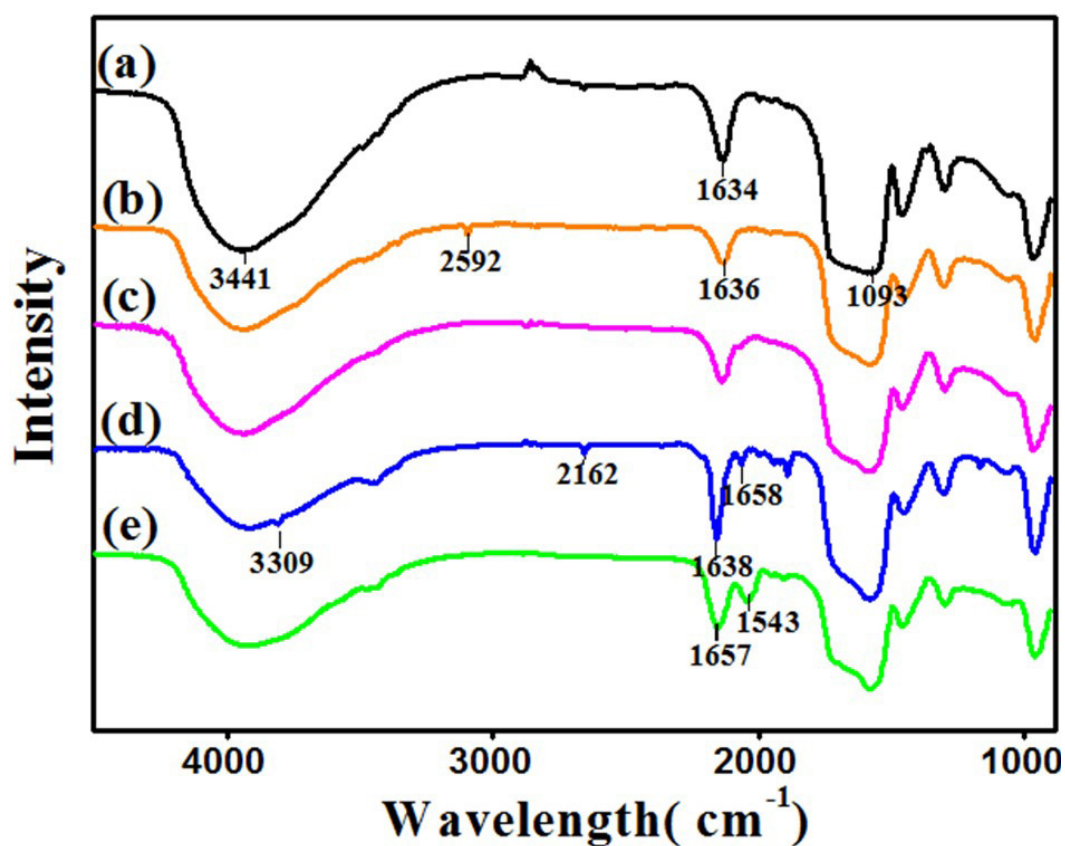
**Figure S3.** Hydrodynamic diameter and polydispersity index (PDI) of HMSNs-S-S-Tf@DOX in saline after four days investigated by DLS.



**Figure S4.** (a) Brunauer-Emmett-Teller (BET) nitrogen adsorption/desorption isotherms and (b) Barrett-Joyner-Halenda (BJH) pore size distribution for HMSNs and the nanoparticles after grafted with functional units step by step.

**Table S2.** BET and BJH measurements for HMSNs before and after grafting with functional groups.

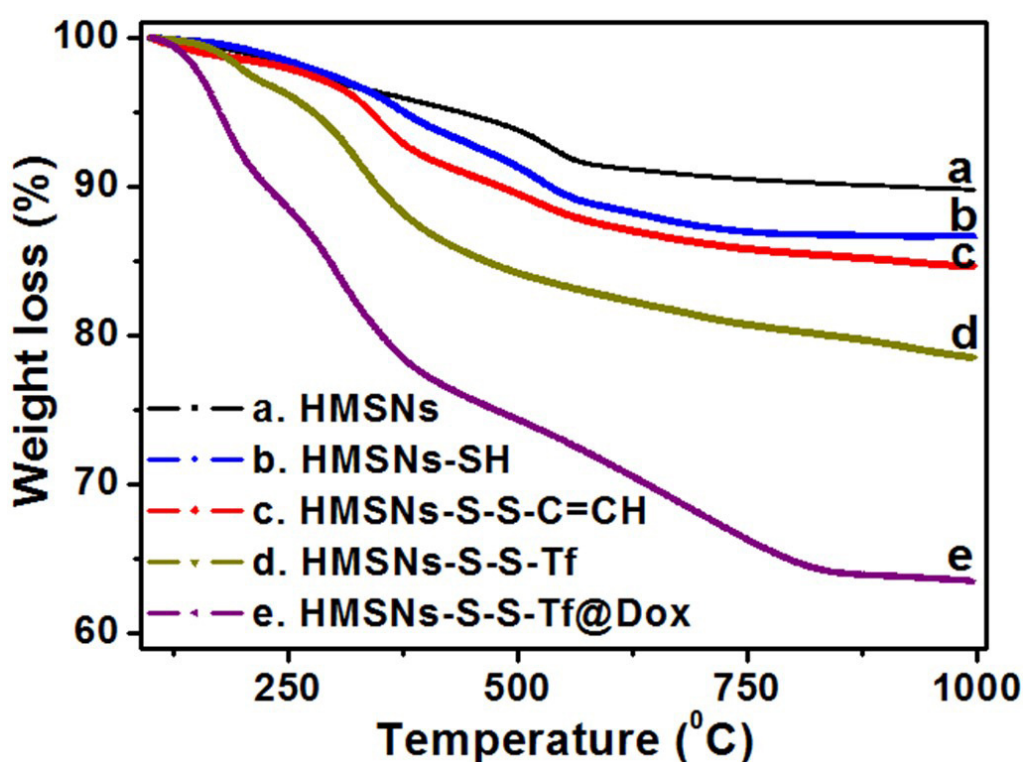
Materials	BET surface area $S_{\text{BET}}$ ( $\text{m}^2/\text{g}$ )	BET pore volume $V_{\text{p}}$ ( $\text{cm}^3/\text{g}$ )	BJH radius pore diameter WBJH (nm)
HMSNs	1297.544	1.1859	2.012
HMSNs-HS	984.563	0.8674	1.985
HMSNs-S-S-C $\equiv$ C	885.164	0.7956	1.971
HMSNs-S-S-Tf	514.865	0.4672	1.965
HMSNs-S-S-Tf@DOX	396.378	0.3376	1.959



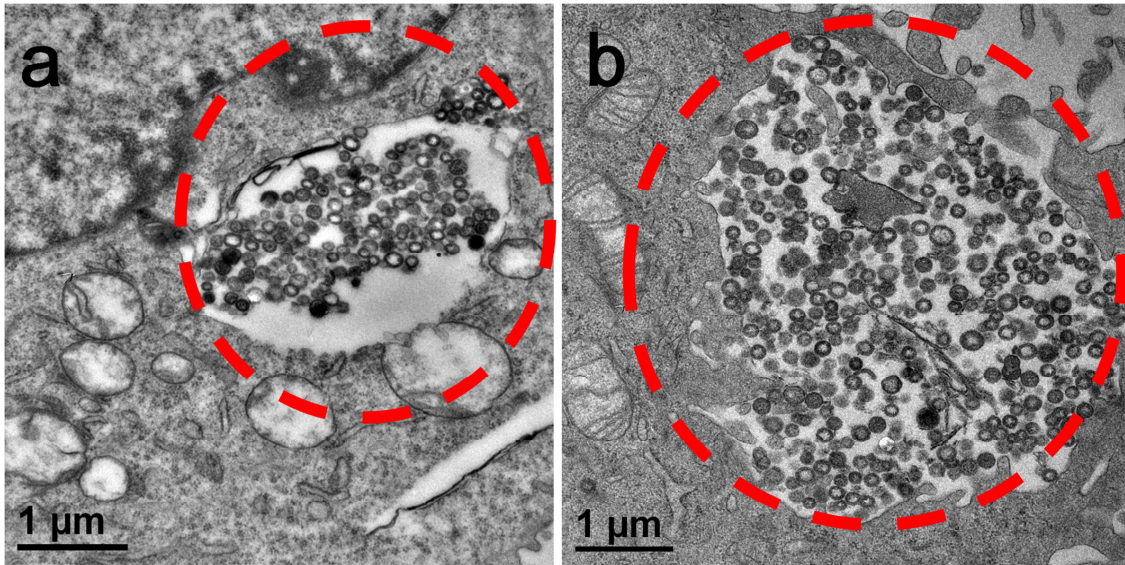
**Figure S5.** FTIR spectra of HMSNs before and after grafting with functional units. FTIR spectra of (a) HMSNs, (b) HMSNs-HS, (c) HMSNs-S-S-COOH, (d) HMSNs-S-S-C $\equiv$ C, and (e) HMSNs-S-S-Tf.

Figure S5 presents the FTIR spectra of different materials. Free HMSNs display a significant absorption signal at  $1093\text{ cm}^{-1}$ , which was ascribed to the asymmetric stretching of the Si-O-Si bonds.<sup>S2</sup> The peak at  $1634\text{ cm}^{-1}$  was attributed to hydroxyl groups in HMSNs (Figure S5a).<sup>S1,S2</sup> After the modification, HMSNs-HS shows a new peak at  $2593\text{ cm}^{-1}$  (Figure S5b), which can be assigned to the stretching vibration of the -HS groups,<sup>S3</sup> indicating that (3-mercaptopropyl) trimethoxysilane (MPTS) was coupled to HMSNs. After modification

with 2-carboxyethyl 2-pyridyl disulfide (Figure S5c), the peak for the –HS group disappeared, since they were consumed during the reaction. This observation suggests that 2-carboxyethyl 2-pyridyl disulfide was functionalized onto HMSNs-HS. After reacting with propargylamine (Figure S5d), some new peaks emerged at  $2162\text{ cm}^{-1}$  and  $1558\text{ cm}^{-1}$  for the sample of HMSNs-S-S-C $\equiv$ C, indicating that alkynyl and amide groups were formed onto the surface of HMSNs, respectively.<sup>S4</sup> Finally, Tf was end-capped onto HMSNs-S-S-C $\equiv$ C *via* the click reaction between alkynyl group in HMSNs-S-S-C $\equiv$ C and azide-conjugated transferrin (Tf-N<sub>3</sub>). Thus, the peak at  $2162\text{ cm}^{-1}$  disappeared, while a new peak appeared at  $1543\text{ cm}^{-1}$  contributed to the stretching of the –NH unit in Tf.<sup>S5</sup> All the results indicate that HMSNs-S-S-Tf was successfully synthesized.



**Figure S6.** Thermogravimetry analysis (TGA) of (a) HMSNs, (b) HMSNs-SH, (c) HMSNs-S-S-C $\equiv$ C, (d) HMSNs-S-S-Tf, and (e) HMSNs-S-S-Tf@DOX.



**Figure S7.** Enlarged TEM images for the identification of the intracellular location of (a) free HMSNs and (b) HMSNs-S-S-Tf after the incubation with breast cancer cells for 24 h. Endocytosed nanoparticles were marked with red circles.

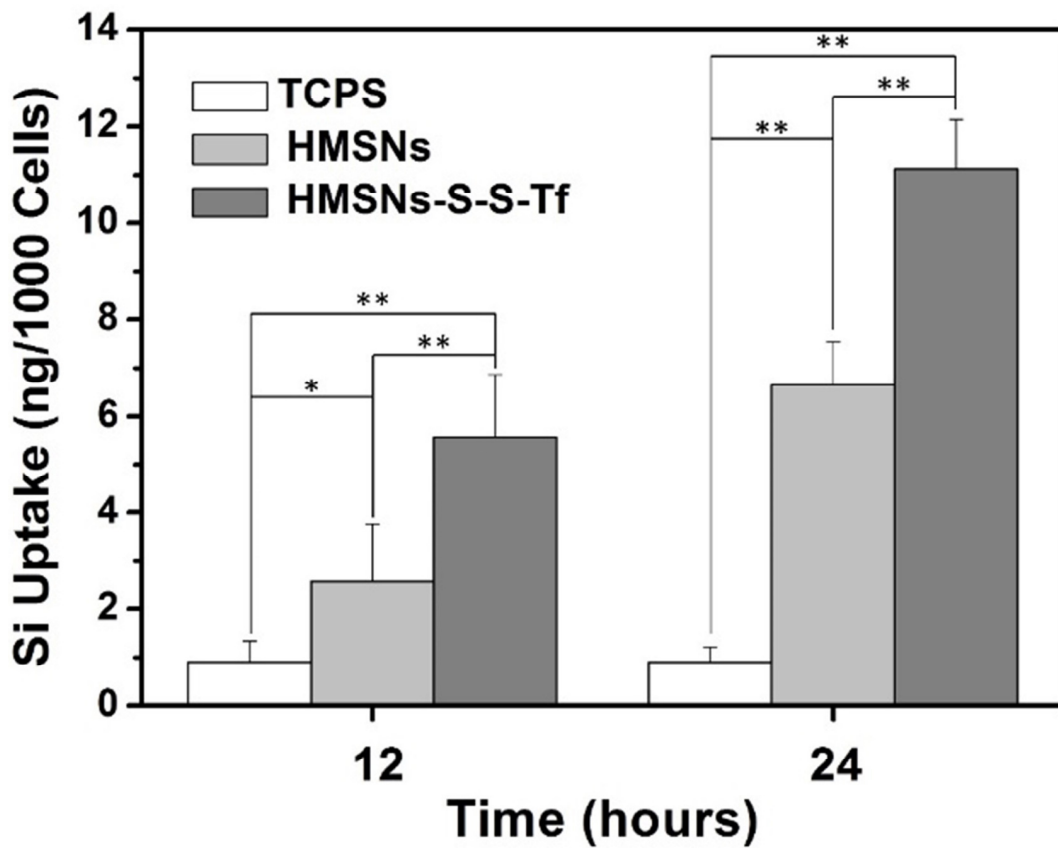


**Figure S8.** Efficiency of endocytosis by MDA-MB-231 cells before and after Tf conjugation, as revealed by ICP analysis.

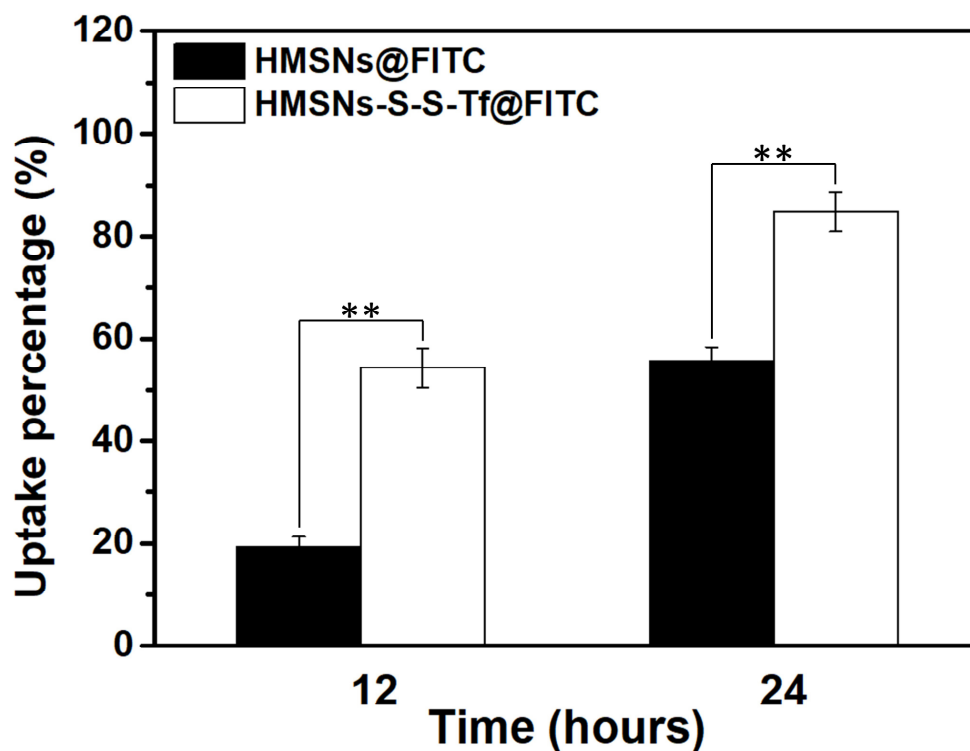


**Figure S9.** Quantitative flow cytometric analysis about the endocytosis percentage of HMSNs@FITC and HMSNs-S-S-Tf@FITC by MDA-MB-231 cells, respectively (n = 6, \*\*p < 0.01).

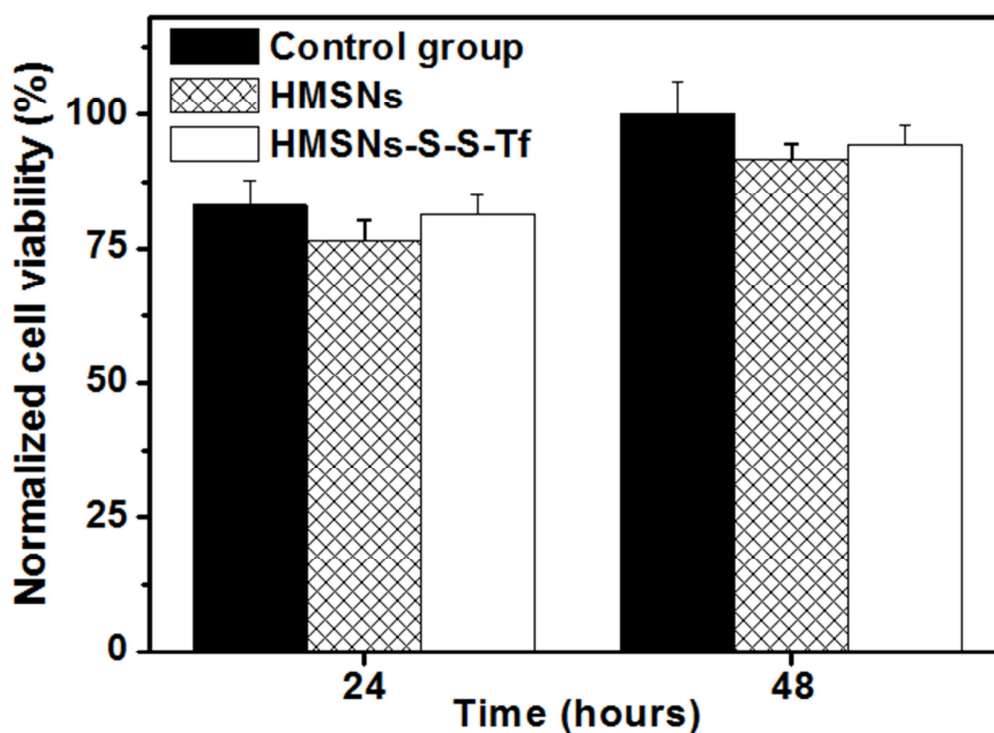


**Figure S10.** Cellular compatibility analysis for HMSNs before and after functionalization as compared with the control group (TCPS).

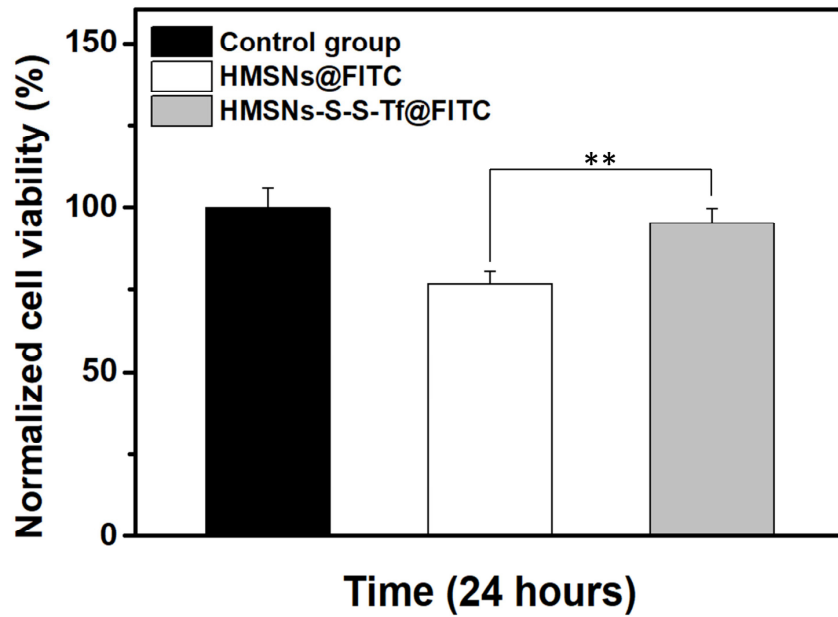


**Figure S11.** RAW 264.7 macrophage cellular compatibility analysis of HMSNs@FITC and HMSNs-S-S-Tf@FITC.

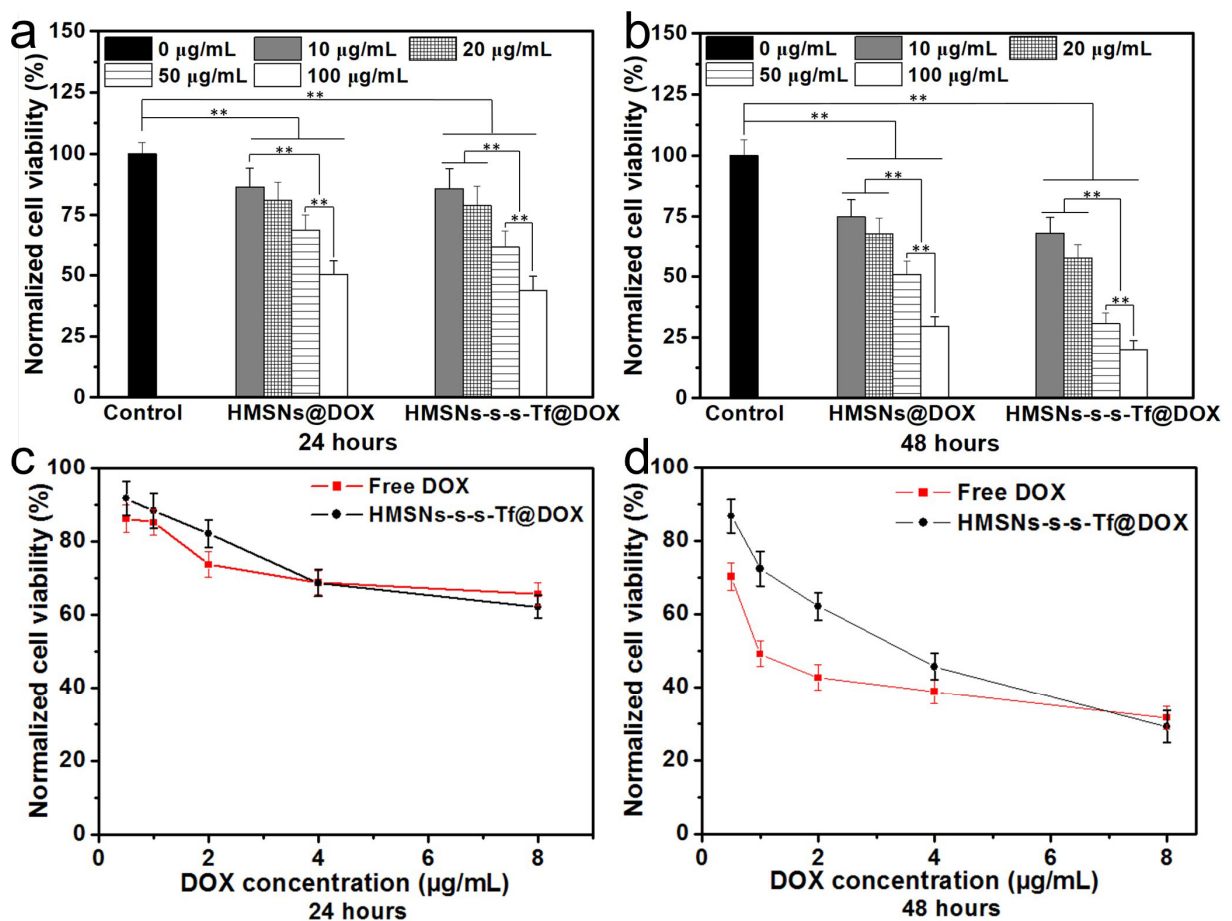


**Figure S12.** Cytotoxic effects of HMSNs@DOX, HMSNs-S-S-Tf@DOX and free DOX on breast cancer cells as compared with the control groups of TCPS and free HMSNs. Incubation time: (a,c) 24 hours and (b,d) 48 hours.



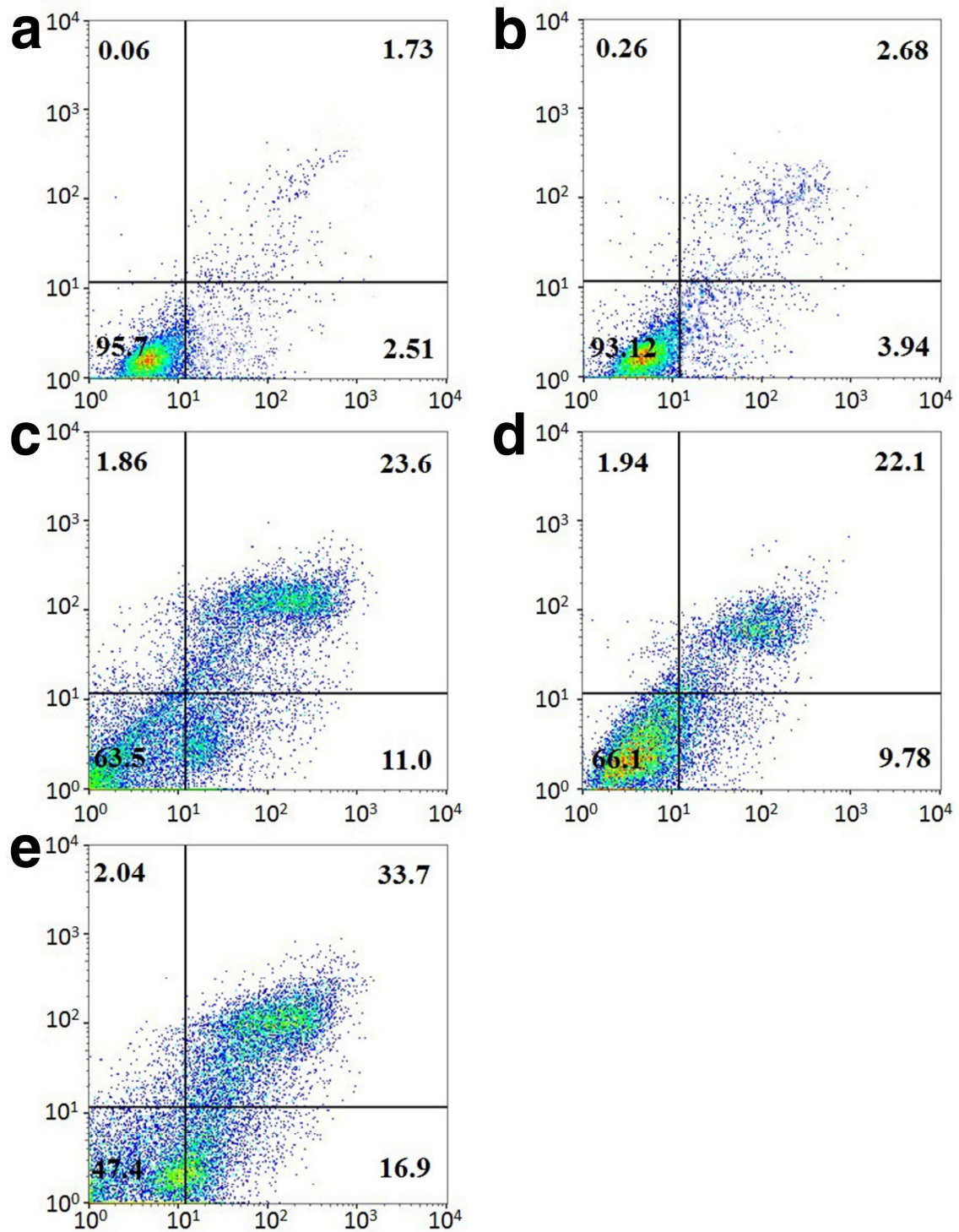


**Figure S13.** Quantitative flow cytometry analysis showing the percentage of apoptotic breast cancer cells after treatment with (a) TCPS, (b) HMSNs, (c) DOX, (d) HMSNs@DOX, and (e) HMSNs-S-S-Tf@DOX respectively. Horizontal axis represents PI intensity, while the vertical axis represents FITC intensity.

**Table S3.** Apoptotic assay of breast cancer cells after the treatment with (a) TCPS, (b) HMSNs, (c) DOX, (d) HMSNs@DOX, and (e) HMSNs-S-S-Tf@DOX. Q1: living cells, Q2: early stage apoptosis cells, Q3: late stage apoptosis cells, Q4: necrosis cells.

	Q1	Q2	Q3	Q4
a	95.7%	2.51%	1.73%	0.06%
b	93.12%	3.94%	2.68%	0.26%
c	63.5%	11.0%	23.6%	1.86%
d	66.1%	9.78%	22.1%	1.94%
e	47.4%	16.9%	33.7%	2.04%

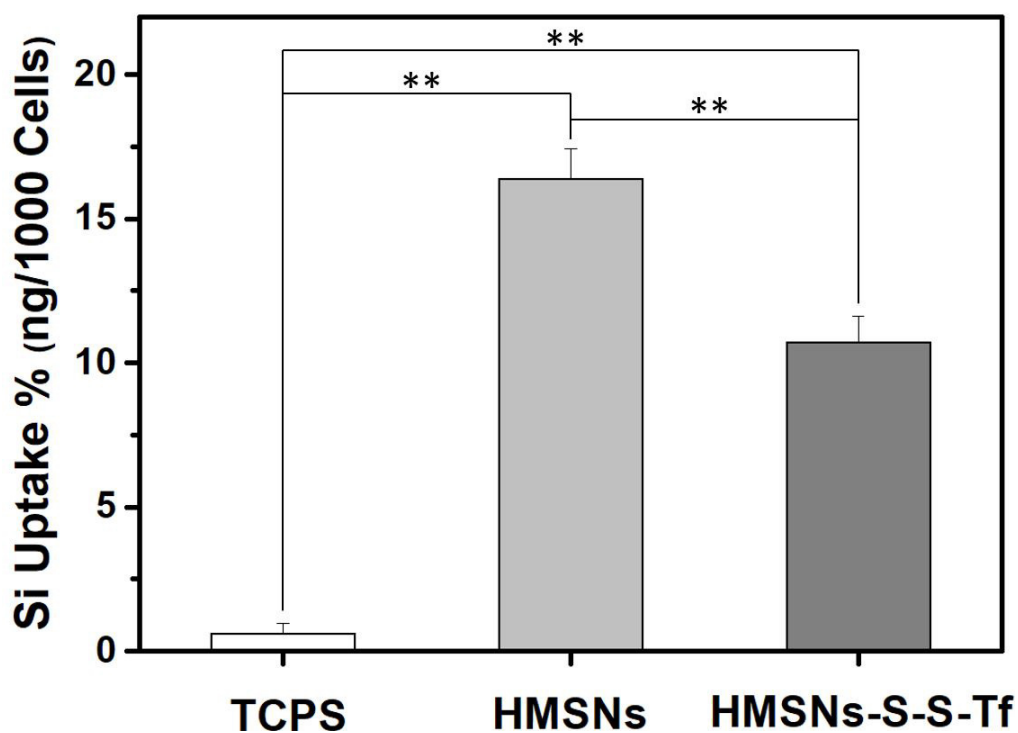


**Figure S14.** ICP characterization for the impact of Tf modification on the macrophage phagocytic efficiency.

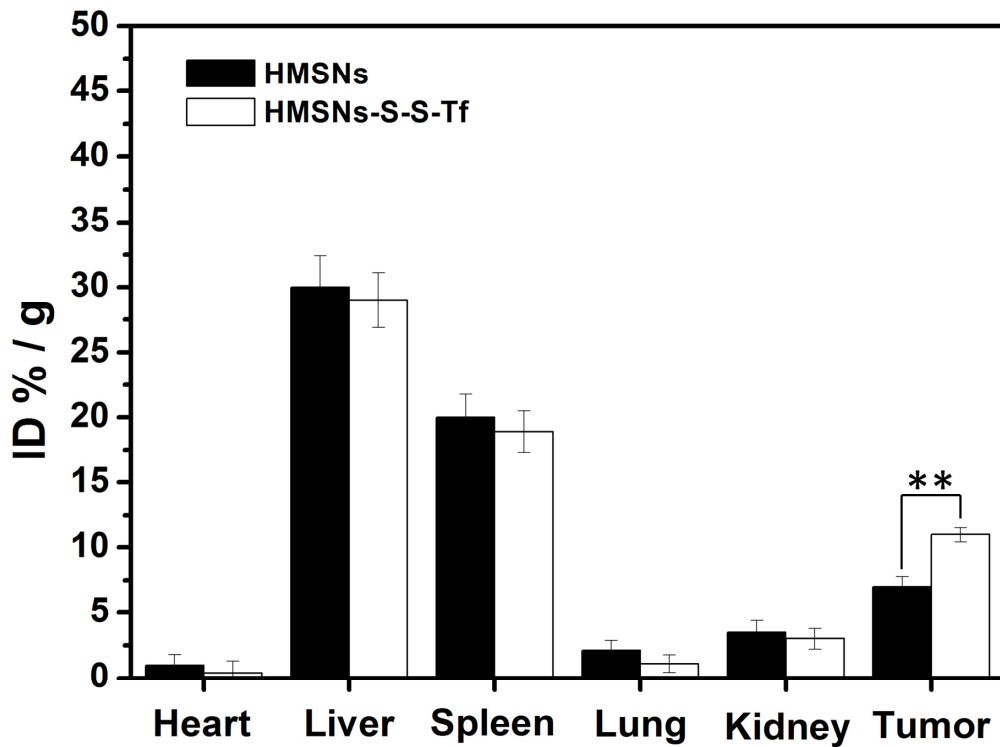


**Figure S15.** Comparison for the distributions of HMSNs and HMSNs-S-S-Tf in major mouse organs and tumors 1 day after intravenous administration.

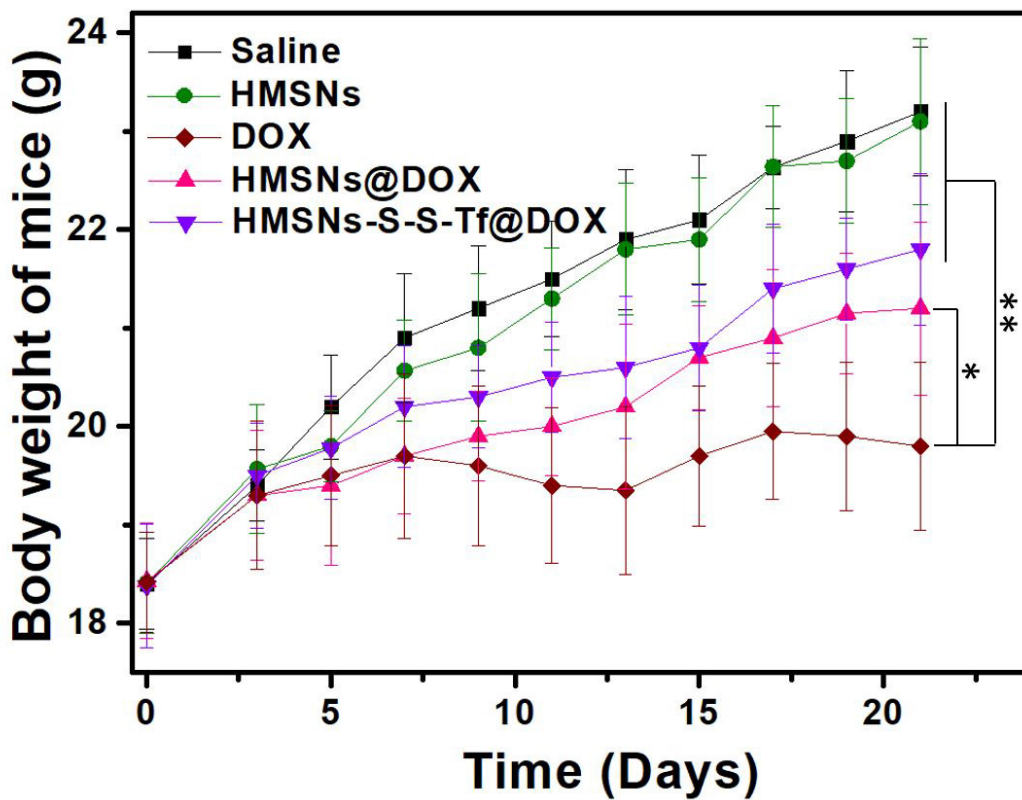


**Figure S16.** Continual monitoring of the weight changes of nude mice after each treatment. Error bars represent means  $\pm$  SD for n=6.

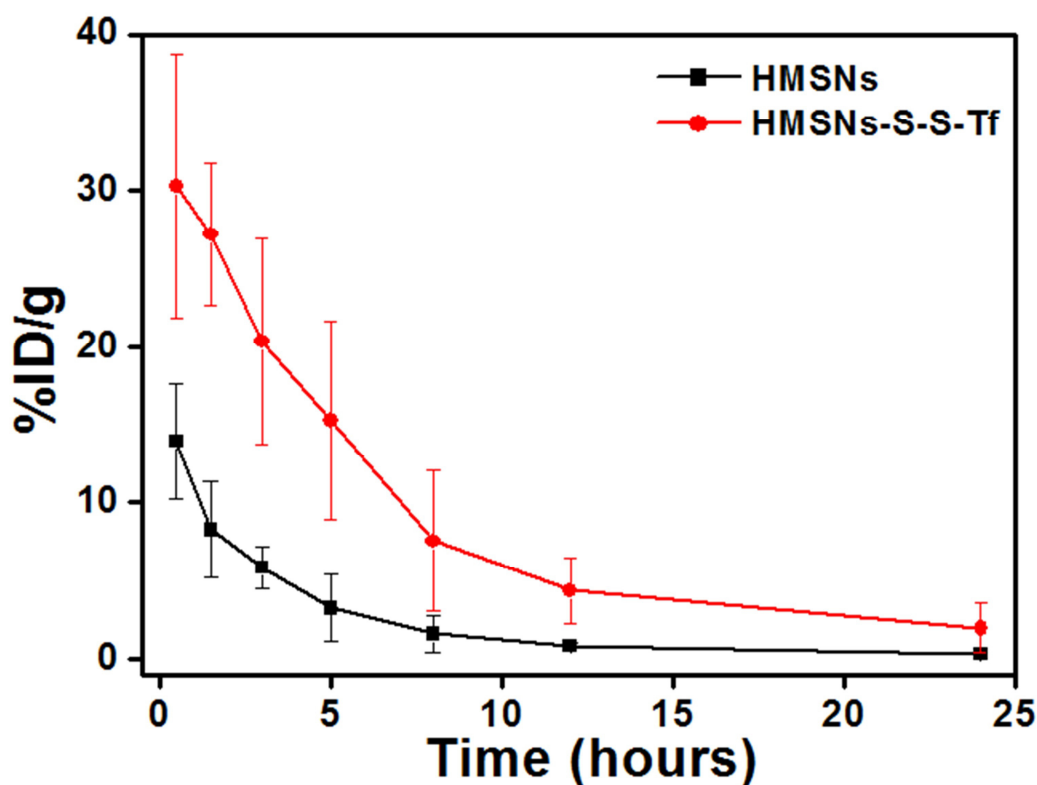


**Figure S17.** Plasma concentration of circulating nanoparticles determined by ICP after the intravenous administration of HMSNs and HMSNs-S-S-Tf.

## References

- S1 Luo Z, Hu Y, Cai K, Ding X, Zhang Q, Li M, Ma X, Zhang B, Zeng Y, Li P, Li J, Liu J, Zhao Y. Intracellular redox-activated anticancer drug delivery by functionalized hollow mesoporous silica manoreservoirs with tumor specificity. *Biomaterials*. 2014;35:7951-7962.
- S2 Luo Z, Ding X, Hu Y, Wu S, Xiang Y, Zeng Y, Zhang B, Yan H, Zhang H, Zhu L, Liu J, Li J, Cai K, Zhao Y. Engineering a hollow nanocontainer platform with multifunctional molecular machines for tumor-targeted therapy in vitro and in vivo. *ACS Nano*. 2013;7:10271-10284.
- S3 Ma X, Nguyen KT, Borah P, Ang CY, Zhao Y. Functional silica nanoparticles for redox-triggered drug/ssDNA co-delivery. *Adv Healthcare Mater*. 2012;1:690-697.
- S4 Yan H, Teh C, Sreejith S, Zhu L, Kwok A, Fang W, Ma X, Nguyen KT, Korzh V, Zhao Y. Functional mesoporous silica nanoparticles for photothermal-controlled drug delivery in vivo. *Angew Chem Int Ed*. 2012;51:8373-8377.
- S5 Ferris DP, Lu J, Gothard C, Yanes R, Thomas CR, Olsen J-C, Stoddart JF, Tamanoi F, Zink JI. Synthesis of biomolecule-modified mesoporous silica nanoparticles for targeted hydrophobic drug delivery to cancer cells. *Small*. 2011;7:1816-1826.